

Provided for non-commercial research and education use.  
Not for reproduction, distribution or commercial use.



(This is a sample cover image for this issue. The actual cover is not yet available at this time.)

This article appeared in a journal published by Elsevier. The attached copy is furnished to the author for internal non-commercial research and education use, including for instruction at the authors institution and sharing with colleagues.

Other uses, including reproduction and distribution, or selling or licensing copies, or posting to personal, institutional or third party websites are prohibited.

In most cases authors are permitted to post their version of the article (e.g. in Word or Tex form) to their personal website or institutional repository. Authors requiring further information regarding Elsevier's archiving and manuscript policies are encouraged to visit:

<http://www.elsevier.com/copyright>



Contents lists available at SciVerse ScienceDirect

## Journal of Luminescence

journal homepage: [www.elsevier.com/locate/jlumin](http://www.elsevier.com/locate/jlumin)

# Superlinear dose response of thermoluminescence (TL) and optically stimulated luminescence (OSL) signals in luminescence materials: An analytical approach

Vasilis Pagonis<sup>a,\*</sup>, Reuven Chen<sup>b</sup>, John L. Lawless<sup>c</sup>

<sup>a</sup> Physics Department, McDaniel College, Westminster, MD 21158, USA

<sup>b</sup> Raymond and Beverly Sackler School of Physics and Astronomy, Tel-Aviv University, Tel-Aviv 69978, Israel

<sup>c</sup> Redwood Scientific Incorporated, Pacifica, CA 94044-4300, USA

## ARTICLE INFO

## Article history:

Received 31 October 2011

Received in revised form

19 December 2011

Accepted 4 January 2012

Available online 24 January 2012

## Keywords:

Thermoluminescence

Optically stimulated luminescence

Superlinearity

Superlinear dose response

Kinetic model

Dose rate effect

## ABSTRACT

The phenomenon of superlinear dose response of thermoluminescence (TL) and optically stimulated luminescence (OSL) signals has been reported for several important dosimetric materials. We develop new analytical equations for the filling of traps and centers during irradiation and for the read-out stage of annealed luminescence materials, within the context of a two-trap and two-center model. The equations are applicable for both TL and OSL signals in annealed dosimetric materials, and are derived under the assumptions of low irradiation doses and dominant strong retrapping (weak recombination) processes. For low doses all traps and centers display linear dose response, which leads to quadratic dose response of the integrated TL/OSL signals. A new analytical expression is presented for this well-known quadratic dose dependence, in terms of the kinetic parameters in the model. The effect of elevated irradiation temperature on the integrated TL/OSL signals is also considered, and analytical expressions are obtained for this situation as well. A new type of dose-rate effect is reported based on the modeling results, which is due to irradiation during elevated temperatures. The accuracy of the analytical expressions is verified by comparing with the results of numerical simulations.

© 2012 Elsevier B.V. All rights reserved.

## 1. Introduction

The phenomenon of superlinear dose response of thermoluminescence (TL) and optically stimulated luminescence (OSL) signals has been reported for several important luminescent materials used in dosimetry and in luminescence dating ([1–8]). In this paper we use the term superlinearity (or supralinearity) to mean faster than linear dependence of the luminescence signal on the dose. In general terms and for certain dose ranges, one writes for the measured TL/OSL signal  $L$  the expression  $L = aD^k$ , where  $D$  is the applied dose,  $a$  is a proportionality factor and  $k$  is a constant. If  $k > 1$  the dependence is termed superlinear, whereas  $k < 1$  means sublinearity and  $k = 1$  means a linear dose dependence. When this behavior takes place in a certain dose range, a plot of  $L$  as a function of  $D$  on a log–log scale is expected to yield a straight line with a slope of  $k$ .

Superlinear dose dependence of the TL signal has been reported in semiconducting diamonds [1],  $\text{CaF}_2:\text{Tb}_4\text{O}_7$  [2],  $\text{Mg}_2\text{SiO}_4:\text{Tb}$  [3,4], for several TL peaks in quartz ([5–8]),  $\text{LiF}:\text{Mg,Ti}$

([9–12]),  $\text{NaCl}:\text{Mg}$  and  $\text{KCl}$  [13], fused silica [14],  $\text{Mg}_2\text{SiO}_4:\text{Tb}$  [15], and carbon doped  $\text{Y}_3\text{Al}_5\text{O}_{12}$  (YAG:C) [16]. There have also been several reports of superlinear dose dependence of OSL signal in quartz and mixed feldspars [17], quartz samples [18], annealed quartz samples from bricks [19], and in  $\text{Al}_2\text{O}_3:\text{C}$  [20].

Several experimental and theoretical/modeling studies have suggested that when one is starting with empty traps and centers in a dosimetric material (as in the case of annealed samples), a quadratic superlinear dose dependence of the integrated TL/OSL signal comes out as a natural result. On the contrary, experimental work shows that linear dose dependence is commonly observed in “as is” samples [17].

In this paper we develop new analytical equations for the trap filling process and for the superlinear dose response of annealed luminescence materials, within the context of a two-trap and two-center model. The equations are applicable for both TL and OSL signals, and are derived under two assumptions. Firstly it is assumed that low irradiation doses are used, i.e. the traps and centers are assumed to be away from saturation. Secondly, it is assumed that the system is dominated by strong retrapping (weak recombination) processes. Good agreement is found between the analytical equations and the numerical solutions of the system of differential equations in the model. At low doses all

\* Corresponding author. Tel.: +1 410 857 2481; fax: +1 410 386 4624.  
E-mail address: [vpagonis@mcDaniel.edu](mailto:vpagonis@mcDaniel.edu) (V. Pagonis).

traps and centers display linear dose response, and this is shown to lead to the well-known quadratic dose dependence of the TL/OSL signals ([21–23] and references therein). A new analytical expression is presented for this quadratic dose dependence, in terms of the kinetic parameters in the model.

The effect of elevated irradiation temperature on the integrated TL/OSL signals is also considered, and analytical expressions are obtained for this situation as well. These analytical expressions can be written in parametric form, and can be used to analyze experimental TL/OSL dose response curves when irradiation of a sample takes place at elevated temperatures.

## 2. Previous theoretical and modeling work of superlinear TL/OSL dose response

There have been several theoretical and modeling attempts to explain various aspects of superlinear dose dependence of TL/OSL signals. For a detailed description of the various proposed models for superlinearity, the reader is referred to the review paper by McKeever and Chen [24], and to the books by Chen and McKeever [21] and Chen and Pagonis [25]. In completely general terms, competition effects between traps and centers in a dosimetric material can explain a wealth of different TL/OSL dose responses. It has been shown that competition during excitation can yield one kind of behavior, while competition during read-out may result in another kind of dependence. In a real material, one can expect to observe the combined effects of both kinds of competition.

Chen and Leung [26] summarized the similarities and dissimilarities between TL and OSL associated with the simple one-trap one-recombination center (OTOR) model. Their simulations and theoretical considerations showed that as long as the trap and recombination center fill linearly with the dose, the dependence of the total area under the TL/OSL curve is expected to be linear within this rather simplistic model. In many materials it is observed that an initial short linear range is followed by a range of superlinearity, which in turn becomes sublinear when approaching saturation. This superlinear behavior can be explained as an effect of competition during excitation, and has been simulated by Chen and Bowman [27]. Kristianpoller et al. [22] showed that the competing trap model can explain the superlinear behavior of TL and OSL signals, under certain assumptions, and provided approximate analytical expressions for the quadratic superlinear dose response demonstrated by several dosimetric materials. Chen and McKeever [28] showed that in the presence of a competing trapping state, a strong superlinearity can be expected, whereas in the presence of a competing non-radiative recombination center, either linear or slightly superlinear dose dependencies can take place.

Chen and Leung [29] also simulated the dose dependence and dose rate dependence of OSL signals using simulations. Banerjee et al. [30,31] simulated the dose dependence of OSL signal from quartz samples, using the comprehensive model by Bailey [32]. Recently Pagonis et al. [33] simulated the superlinear dose dependence of the TL/OSL signals from quartz using a comprehensive model consisting of 11 energy levels. They showed that the quadratic superlinear behavior of the TL/OSL signals can be removed by correcting the luminescence signals for sensitivity changes, as is done routinely during geological and archeological dating applications.

Chen and Leung [29] have also modeled the situation where one of the trapping states involved is nearly full of carriers at the onset of the experiment. From a theoretical point of view, if the quadratic dose dependence is associated with the product of occupancies of electrons in traps and holes in centers, having one

of them practically constant might bring about a linear dependence of the TL/OSL intensity on the dose, if the other occupancy is linear with the dose. In their simulations Chen and Leung [29] assumed that the dosimetric trap is 90% full before irradiation. In this situation they found that the dose dependence of the TL/OSL signal is indeed linear.

Other notable contributions concerning the quadratic and more-than-quadratic dose dependence are those by Savikhin [34], Zavt and Savikhin [35] and by Kantorovich et al. [36]; the quadratic dose dependence due to competition during heating was also discussed by Sunta et al. [37]. Additional theoretical studies of the dose dependence of TL when competition takes place during heating were presented by Mady et al. [38], Faïn and Monnin [39] and Faïn et al. [40], who explained the behavior of a superlinear dose dependence following a linear range on a different physical basis.

## 3. The model

We use a simple energy level model consisting of two electron traps  $T$  and  $S$ , a luminescence center  $L$  and a hole reservoir  $R$ , as shown in Fig. 1. This type of model has been used successfully to simulate the dose response of several important materials, such as quartz and  $\alpha\text{-Al}_2\text{O}_3\text{:C}$  ([21,41–49]). The results from this model will include the cases of the OTOR, two-trap-one-center (2T1C) and one-trap-two-centers (1T2C) models previously considered in the literature.

The transitions shown in Fig. 1 are during the excitation and during the read-out stages.  $T$  is the active dosimetric trapping state having a total concentration of  $N_t$  ( $\text{cm}^{-3}$ ) and an instantaneous occupancy  $n_t$  ( $\text{cm}^{-3}$ ); the corresponding activation energy is  $E_t$  (eV) and the frequency factor  $s_t$  ( $\text{s}^{-1}$ ).  $S$  is a thermally disconnected trapping state with concentration  $N_s$  ( $\text{cm}^{-3}$ ) and occupancy of  $n_s$  ( $\text{cm}^{-3}$ ).  $A_t$  ( $\text{cm}^3 \text{s}^{-1}$ ) and  $A_s$  ( $\text{cm}^3 \text{s}^{-1}$ ) are the trapping coefficients into  $T$  and  $S$  respectively.  $L$  is the luminescence center with concentration  $M$  ( $\text{cm}^{-3}$ ) and instantaneous occupancy of  $m$  ( $\text{cm}^{-3}$ ). The transition coefficient of the free holes from the valence band into  $L$  is  $A_l$  ( $\text{cm}^3 \text{s}^{-1}$ ) and the recombination coefficient of free holes is  $A_m$  ( $\text{cm}^3 \text{s}^{-1}$ ).  $R$  is the hole reservoir having a concentration of  $N_r$  ( $\text{cm}^{-3}$ ) and instantaneous occupancy of  $n_r$  ( $\text{cm}^{-3}$ );  $E_r$  (eV) is the activation energy of releasing holes from  $R$  thermally into the valence band and  $s_r$  ( $\text{s}^{-1}$ ) the relevant frequency factor. The rate at which electron-hole pairs are produced by the irradiation is  $x$  ( $\text{cm}^{-3} \text{s}^{-1}$ ) which is proportional to the dose rate imparted on the sample. Thus, if the irradiation time is  $t_D$ , the total dose given to the sample is

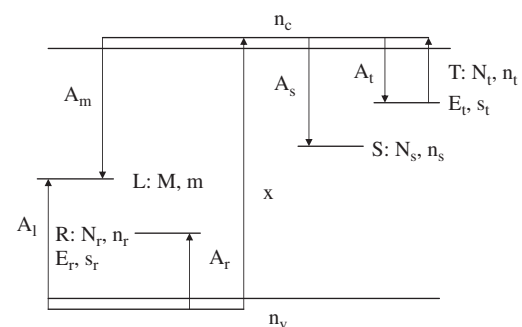


Fig. 1. An energy-level diagram including the electron trapping state,  $T$ , the competitor,  $S$ , the hole reservoir,  $R$  and the luminescence center  $L$ .  $n_c$  and  $n_v$  are the free electron and hole concentrations, respectively, and  $x$  is the rate of production of free electrons and holes. The transitions taking place both during excitation and heating are shown.

proportional to  $D=xt_D$  ( $\text{cm}^{-3}$ ), which is the number of electrons and holes produced by the irradiation per unit volume.

The simulation consists of the following stages. The final concentrations of the traps and centers at the end of each stage are used as the initial values for the next stage in the simulation. Appropriate relaxation intervals are included between the stages in order to allow the concentrations of electrons and holes in the conduction and valence band to reach zero.

STAGE I: All initial concentrations of traps and centers are set at zero, as would be the case for an annealed dosimetric material. The sample is irradiated for an irradiation time  $t_D$ , and the total dose given to the sample is proportional to  $D=xt_D$  ( $\text{cm}^{-3}$ ), as described above.

STAGE II: The sample is heated up to a low temperature of 200 °C in order to empty the dosimetric trap  $T$ , and to measure the TL signal  $L$ . Alternatively, if  $T$  is an optically sensitive trap, the sample would be optically stimulated at room temperature in order to empty  $T$ , and  $L$  will denote the OSL signal in this case. The equations derived in this paper are valid for both optical and thermal stimulation of electrons in trap  $T$ .

The above process consisting of stages I and II is repeated for different irradiation times  $t_D$ , in order to obtain the dose response of the TL/OSL signal at different doses  $D$ .

In order to facilitate the notation, we denote the concentrations of traps and centers at the end of each stage, by the corresponding Latin numeral. For example, we denote the concentration of electrons and holes in  $T$ ,  $S$ ,  $L$  and  $R$  at the end of STAGE I by the symbols  $(n_t)_I$ ,  $(n_s)_I$ ,  $m_I$  and  $(n_r)_I$  correspondingly. Similarly we use the symbols  $(n_t)_{II}$ ,  $(n_s)_{II}$ ,  $m_{II}$  and  $(n_r)_{II}$  for the concentrations at the end of stage II, etc.

It is also noted that the model in Fig. 1 was initially developed to explain the predose effect in quartz, during which thermal release of holes from the reservoir  $R$  into the valence band plays a key role (see for example, [41,42,46]). In the following discussion and simulations,  $R$  plays simply the role of a competitor to the luminescence center  $L$  for capturing holes from the valence band during irradiation. It is assumed that there is no thermal release of holes from  $R$  at the relatively low temperatures used in the simulations of this paper.

### 3.1. Stage I: irradiation of the sample at room temperature

The set of equations governing the process during the excitation stage is

$$dn_t/dt = A_t n_c (N_t - n_t), \quad (1)$$

$$dn_s/dt = A_s n_c (N_s - n_s), \quad (2)$$

$$dn_v/dt = x - A_t n_v (M - m) - A_r n_v (N_r - n_r), \quad (3)$$

$$dm/dt = A_t n_v (M - m) - A_m m n_c, \quad (4)$$

$$dn_r/dt = A_r n_v (N_r - n_r), \quad (5)$$

$$dn_c/dt = x - A_m m n_c - A_t n_c (N_t - n_t) - A_s n_c (N_s - n_s). \quad (6)$$

After a short initial transient time interval, the concentrations  $n_c$  and  $n_v$  reach equilibrium, and we can set  $dn_c/dt=0$  and  $dn_v/dt=0$ . From Eq. (6) we obtain

$$dn_c/dt = 0 = x - A_m m n_c - A_t n_c (N_t - n_t) - A_s n_c (N_s - n_s), \quad (7)$$

$$n_c = \frac{x}{A_m m + A_t (N_t - n_t) + A_s (N_s - n_s)}. \quad (8)$$

The equations in this paper are derived under two assumptions: all levels are far from saturation, i.e.  $n_t \ll N_t$ ,  $n_s \ll N_s$ ,  $m \ll M$ ,

$n_r \ll N_r$  and furthermore we assume that we have weak recombination i.e.  $A_m m \ll A_s N_s + A_t N_t$  at all irradiation times  $t$ .

Under these assumptions Eq. (8) simplifies to

$$n_c = \frac{x}{A_t N_t + A_s N_s}. \quad (9)$$

Similarly from Eq. (3) we obtain

$$dn_v/dt = 0 = x - A_t n_v (M - m) - A_r n_v (N_r - n_r), \quad (10)$$

$$n_v = \frac{x}{A_r N_r + A_t M}. \quad (11)$$

Using Eqs. (9) and (11) we will derive analytical expressions for the concentrations of traps and centers during the irradiation process. From Eqs. (1) and (9) we find

$$dn_t/dt = A_t n_c (N_t - n_t) \simeq A_t n_c N_t = \frac{x A_t N_t}{A_t N_t + A_s N_s}, \quad (12)$$

with the linear solution:

$$n_t(t) = \frac{A_t N_t}{A_m m + A_t N_t + A_s N_s} x t. \quad (13)$$

Similarly from Eq. (2) and (5) we obtain

$$n_s(t) = \frac{A_s N_s}{A_t N_t + A_s N_s} x t, \quad (14)$$

$$n_r(t) = \frac{A_r N_r}{A_r N_r + A_t M} x t. \quad (15)$$

From Eq. (4) we obtain

$$dm/dt = A_t n_v (M - m) - A_m m n_c \simeq A_t n_v M - A_m m n_c. \quad (16)$$

Substituting from Eqs. (9) and (11):

$$dm/dt = \frac{A_t M x}{A_r N_r + A_t M} - \frac{A_m m x}{A_t N_t + A_s N_s}. \quad (17)$$

For low doses and for weak recombination, the second term in this equation is much smaller than the first term, therefore Eq. (17) also yields a linear dose dependence for the recombination center  $L$ :

$$m(t) = \frac{A_t M}{(A_r N_r + A_t M)} x t. \quad (18)$$

It is concluded that during the irradiation process and under weak recombination conditions and for low doses, the concentrations of carriers in  $T$ ,  $S$ ,  $L$  and  $R$  will increase linearly with time  $t$ , and therefore also linearly with the dose  $D=xt$ . In the next section it is shown that these linear dose responses lead to quadratic superlinearity of the integrated TL/OSL signal during the heating stage, and an analytical equation will be derived for this quadratic dose response.

### 3.2. Stage II: heating of the sample—superlinearity

A second part of the simulation deals with the transitions taking place during the heating of the sample, with the corresponding transitions also shown in Fig. 1.

At the end of the natural irradiation stage of duration  $t_D$ , the  $D=xt_D$  electrons produced during irradiation will be trapped at  $T$ ,  $S$  and  $L$  in proportion to their corresponding trapping probabilities  $A_t(N_t - n_t)$ ,  $A_s(N_s - n_s)$  and  $A_m m$ . By assuming that these levels are far from saturation, i.e.  $n_t \ll N_t$ ,  $n_s \ll N_s$ ,  $m \ll M$  and furthermore that strong retrapping (weak recombination) dominates, i.e.  $A_m m \ll A_s N_s + A_t N_t$ , the concentrations of trapped electrons at  $T$  and  $S$  at the end of stage I will be

$$(n_t)_I = D \frac{A_t N_t}{A_t N_t + A_s N_s}, \quad (19)$$

$$(n_s)_I = D \frac{A_s N_s}{A_t N_t + A_s N_s}, \quad (20)$$

where  $D = xt_D$  is the concentration of electrons produced during irradiation.

During the same time interval, the holes created in the valence band, will distribute themselves between the luminescence center  $L$  and the hole reservoir  $R$ , in proportion to the corresponding trapping probabilities. By assuming again that  $R$  and  $L$  are far from saturation, i.e.  $m \ll M$ ,  $n_r \ll N_r$  we obtain

$$(m)_I = D \frac{A_l M}{A_r N_r + A_l M}, \quad (21)$$

$$(n_r)_I = D \frac{A_r N_r}{A_r N_r + A_l M}. \quad (22)$$

Eqs. (19)–(22) are of course identical to the Eqs. (13–15) and (18) derived previously, with  $D = xt_D$ .

During the heating process up to e.g. 200 °C, the rate equations governing the process are

$$dn_t/dt = A_t n_c (N_t - n_t) - s_t n_t \exp(-E_t/kT), \quad (23)$$

$$dn_s/dt = A_s n_c (N_s - n_s), \quad (24)$$

$$dn_v/dt = n_r s_r \exp(-E_r/kT) - A_r n_v (N_r - n_r) - A_l n_v (M - m), \quad (25)$$

$$dm/dt = A_l n_v (M - m) - A_m n_c m, \quad (26)$$

$$dn_r/dt = A_r n_v (N_r - n_r) - n_r s_r \exp(-E_r/kT), \quad (27)$$

$$dn_c/dt = -A_m m n_c - A_t n_c (N_t - n_t) - A_s n_c (N_s - n_s) + s_t n_t \exp(-E_t/kT). \quad (28)$$

The choice of the maximum read-out temperature as 200 °C is rather arbitrary, and was chosen to correspond closely to the temperature commonly used during the predose effect of quartz. This maximum read-out temperature will of course be different for other materials, or for deeper dosimetric traps. The numerical example given in the paper uses also values of the kinetic parameters  $E_t, s_t$  which are consistent with the values for the 110 °C TL trap of quartz. For the relatively low temperatures used in this paper, we can assume that the thermal release term for holes  $n_r s_r \exp(-E_r/kT)$  in Eqs. (25) and (27) is negligible, i.e. that no holes are released thermally from the hole reservoir  $R$ . The intensity of the emitted light is assumed to be the result of recombination of free electrons with trapped holes in the centers. Therefore, it is given by

$$I(T) = A_m m n_c. \quad (29)$$

In the simulation, a conventional linear heating function is used,  $T(t) = T_0 + \beta t$  where  $\beta$  is the constant heating rate chosen to be 5 °C/s. Alternatively, if trap  $T$  is optically sensitive, it can be emptied by optical stimulation of the appropriate duration. Mathematically one would then replace the thermal excitation term  $-s_t n_t \exp(-E_t/kT)$  in Eq. (23), with an optical excitation term  $-\lambda n_t$ . Here  $\lambda = \sigma I$  is the probability of optical excitation in  $s^{-1}$ , which is a constant proportional to the light intensity  $I$  (photons  $cm^{-2} s^{-1}$ ) and to the optical excitation cross section  $\sigma$  ( $cm^2$ ) of the material. Since we are only concerned with the total integrated TL/OSL intensity, the equations derived in this paper are valid for both thermal and optical excitation.

During the heating stage II up to a temperature  $T = 200$  °C, trap  $T$  is emptied thermally, while trap  $S$  is assumed to be thermally stable within this temperature range. The initial concentration  $(n_t)_I$  of electrons in trap  $T$  is given by the expression in Eq. (19); these electrons are thermally or optically released into the CB during the heating stage, and are redistributed between  $L$  and  $S$ , according to the corresponding trapping probabilities.

It is assumed that due to the weak recombination conditions, the number of electrons trapped into  $L$  during stage II is very small, and therefore trapping of these electrons does not alter significantly the number of trapped holes  $m_I$  at the luminescence center. It is also assumed that there is no effect on the concentration of holes in  $R$ , due to the low temperatures used during the heating stage. Under these assumptions, the carrier concentrations at the end of heating stage II will be

$$(n_t)_{II} \approx 0, \quad (30)$$

$$(m)_{II} \approx (m)_I, \quad (31)$$

$$(n_r)_{II} \approx (n_r)_I. \quad (32)$$

The concentration of electrons captured in the competitor trap  $S$  will increase according to

$$(n_s)_{II} = (n_s)_I + (n_t)_I \frac{A_s N_s}{A_m m + A_t N_t + A_s N_s}. \quad (33)$$

By using Eqs. (19) and (20) in this equation we find

$$(n_s)_{II} = D \frac{A_s N_s}{A_t N_t + A_s N_s} + D \frac{A_t N_t}{A_t N_t + A_s N_s} = D, \quad (34)$$

which could also have been expected on the basis of conservation of charge.

The validity of the assumption  $(m)_{II} = (m)_I$  is also checked within the numerical simulations presented in a subsequent section of this paper.

The luminescence signal measured at this heating stage II, is the small portion of  $(n_t)_I$  captured in  $L$ , i.e.

$$L = (n_t)_I \frac{A_m (m)_{II}}{A_s N_s + A_m (m)_{II}}, \quad (35)$$

or by using Eqs. (19) and (31):

$$L = D \frac{A_t N_t}{A_t N_t + A_s N_s} \frac{A_m (m)_I}{A_s N_s + A_m (m)_I}. \quad (36)$$

By substituting  $(m)_I$  from Eq. (21) into (36), we find

$$L = D \frac{A_t N_t}{A_t N_t + A_s N_s} \frac{A_m D [A_l M / (A_r N_r + A_l M)]}{A_s N_s + A_m D [A_l M / (A_r N_r + A_l M)]}, \quad (37)$$

which can be written more clearly as

$$L = D^2 \frac{A_t N_t}{A_t N_t + A_s N_s} \frac{A_m [A_l M / (A_r N_r + A_l M)]}{A_s N_s + A_m D [A_l M / (A_r N_r + A_l M)]}. \quad (38)$$

The last expression in Eq. (38) depends on the dose  $D$  in a non-linear manner. It is also noted that Eq. (38) is applicable for both integrated TL and OSL dose response, since no assumption is made whether the electrons in  $T$  are released thermally or optically from this dosimetric trap.

We summarize that the only two assumptions made in deriving Eq. (38) are that firstly all levels are far from saturation, i.e.  $n_t \ll N_t$ ,  $n_s \ll N_s$ ,  $n_r \ll N_r$ ,  $m \ll M$ , and secondly that the condition  $A_m m \ll A_s N_s + A_t N_t$  is satisfied.

If in addition to these conditions we assume that

$$A_s N_s \gg A_m D \frac{A_l M}{A_r N_r + A_l M} = A_m m_I \quad (39)$$

then the last term in Eq. (38) can be approximated to be constant, and Eq. (38) yields the quadratic dose response for the luminescence signal:

$$L = D^2 \frac{A_t N_t}{A_t N_t + A_s N_s} \frac{A_m A_l M}{A_s N_s (A_r N_r + A_l M)}. \quad (40)$$

This is the desired equation, expressing the quadratic dose dependence of the TL/OSL signal in analytical form.

It is noted that by inserting  $N_r = 0$  in Eqs. (38) or (40), one still obtains similar expressions and the same type of dose behavior.

This indicates that the presence of the hole reservoir  $R$  in the model does not affect the behavior of the luminescence signal as a function of the dose  $D$ , but only affects the overall magnitude of the luminescence signal in these expressions. As the total concentration  $N_r$  increases, one obtains a smaller signal  $L$ , due to competition for holes between the hole reservoir  $R$  and the luminescence center during irradiation of the sample.

#### 4. Irradiation at elevated temperatures

In this section we consider the possibility of carrying out the sample irradiation at an elevated temperature, and study the effects of this elevated temperature on the trap filling process.

By elevated temperatures in this section it is meant that the irradiation stage is carried out at a temperature higher than RT.

During irradiation at elevated temperatures, electrons will escape thermally into the conduction band, a process described by a term of the form  $s_t n_t \exp(-E_t/kT)$ , where  $s_t$  and  $E_t$  are the frequency factor and activation energy for trap  $T$ . The numerical values for the kinetic parameters  $s_t$ ,  $E_t$  of the dosimetric trap in the model are chosen such that this trap is thermally stable at room temperature. However, when irradiation of the sample is carried out above room temperature, the occupancies of the various levels will depend on the value of this irradiation temperature  $T_{irr}$ .

When the irradiation is carried out at an elevated temperature  $T_{irr}$ , the set of coupled differential equations governing the process is

$$dn_t/dt = A_t n_c (N_t - n_t) - s_t n_t \exp(-E_t/kT_{irr}), \quad (41)$$

$$dn_s/dt = A_s n_c (N_s - n_s), \quad (42)$$

$$dn_v/dt = x - A_t n_v (M - m) - A_r n_v (N_r - n_r), \quad (43)$$

$$dm/dt = A_t n_v (M - m) - A_m m n_c, \quad (44)$$

$$dn_r/dt = A_r n_v (N_r - n_r). \quad (45)$$

The traffic of electrons through the CB is described by the equation

$$dn_c/dt = x - A_m m n_c - A_t n_c (N_t - n_t) - A_s n_c (N_s - n_s) + s_t n_t \exp(-E_t/kT_{irr}). \quad (46)$$

After a short transient time interval, equilibrium is reached and by setting  $dn_c/dt=0$  we obtain

$$dn_c/dt = 0 = x - A_m m n_c - A_t n_c (N_t - n_t) - A_s n_c (N_s - n_s) + s_t n_t \exp(-E_t/kT_{irr}). \quad (47)$$

Solving this equation for  $n_c$  and using the previous approximations  $n_t \ll N_t$ ,  $n_s \ll N_s$ ,  $n_r \ll N_r$ ,  $m \ll M$ ,  $A_m m \ll A_s N_s + A_t N_t$ :

$$n_c = \frac{x + s_t n_t \exp(-E_t/kT_{irr})}{A_m m + A_t (N_t - n_t) + A_s (N_s - n_s)} = \frac{x + s_t n_t \exp(-E_t/kT_{irr})}{A_t N_t + A_s N_s}. \quad (48)$$

We now replace this value of  $n_c$  into Eq. (41) to find

$$dn_t/dt = A_t n_c N_t - s_t n_t \exp(-E_t/kT_{irr}) = A_t N_t \frac{x + s_t n_t \exp(-E_t/kT_{irr})}{A_t N_t + A_s N_s} - s_t n_t \exp(-E_t/kT_{irr}). \quad (49)$$

The solution for this equation is a saturating exponential function:

$$n_t(t) = \frac{A_t N_t x}{A_s N_s s_t \exp(-E_t/kT_{irr})} (1 - e^{-(A_s N_s s_t \exp(-E_t/kT_{irr}) / (A_t N_t + A_s N_s)) t}). \quad (50)$$

This equation describes how the dosimetric trap  $T$  fills with time, when irradiation is taking place at a higher temperature  $T_{irr}$ . We note that  $n_t(t)$  depends only on the parameters  $N_s$ ,  $A_s$ ,  $N_t$ ,  $A_t$  as

might be expected from the competition process between the main trap  $T$  and the competitor trap  $S$ .

For short times  $t$ , i.e. when

$$\frac{A_s N_s s_t \exp(-E_t/kT_{irr})}{A_t N_t + A_s N_s} t \ll 1, \quad (51)$$

this gives a linear expression

$$n_t(t) = \frac{A_t N_t x}{A_s N_s s_t \exp(-E_t/kT_{irr})} \frac{A_s N_s s_t \exp(-E_t/kT_{irr})}{A_t N_t + A_s N_s} t = \frac{A_t N_t}{A_s N_s} x t. \quad (52)$$

This equation says that the irradiation temperature has no effect at short times or very small doses, a rather surprising result. The concentration  $n_s(t)$  is found by substituting  $n_c$  from Eq. (48) into Eq. (42):

$$dn_s/dt = A_s n_c (N_s - n_s) \simeq A_s n_c N_s = A_s N_s \frac{x + s_t n_t \exp(-E_t/kT_{irr})}{A_t N_t + A_s N_s}. \quad (53)$$

Substituting the expression for  $n_t(t)$  from Eq. (50) we find

$$dn_s/dt = A_s N_s \frac{x + (A_t N_t x / A_s N_s) (1 - e^{-(A_s N_s s_t \exp(-E_t/kT_{irr}) / (A_t N_t + A_s N_s)) t})}{A_t N_t + A_s N_s}, \quad (54)$$

$$dn_s/dt = x \frac{A_s N_s + A_t N_t (1 - e^{-(A_s N_s s_t \exp(-E_t/kT_{irr}) / (A_t N_t + A_s N_s)) t})}{A_t N_t + A_s N_s}. \quad (55)$$

The solution of this differential equation with  $n_s(0)=0$  is

$$n_s(t) = \frac{x}{A_s N_s \gamma} \left[ A_t N_t (e^{-(A_s N_s \gamma) / (A_t N_t + A_s N_s) t} - 1) + A_s N_s \gamma t \right], \quad (56)$$

where

$$\gamma = s_t \exp(-E_t/kT_{irr}). \quad (57)$$

Eq. (56) describes how the competitor trap  $S$  fills with irradiation time  $t$  at elevated temperatures, and contains a linear term which increases with time  $t$ , and an exponential term which decreases for large irradiation times  $t$ .

The luminescence signal  $L$  measured after the end of this higher temperature irradiation will be found once more from Eq. (35), by substituting the value of  $n_t(t)$  from Eq. (50):

$$L = (n_t)_I \frac{A_m(m)_{II}}{A_s N_s + A_m(m)_{II}} = \frac{A_t N_t x}{A_s N_s s_t \exp(-E_t/kT_{irr})} (1 - e^{-(A_s N_s s_t \exp(-E_t/kT_{irr}) / (A_t N_t + A_s N_s)) t}) \frac{A_m(m)_{II}}{A_s N_s + A_m(m)_{II}}. \quad (58)$$

Next by substituting the value of  $(m)_{II}=(m)_I$  from Eq. (37), we find

$$L = \frac{A_t N_t x}{A_s N_s s_t \exp(-E_t/kT_{irr})} (1 - e^{-(A_s N_s s_t \exp(-E_t/kT_{irr}) / (A_t N_t + A_s N_s)) t}) \times \frac{A_m D [A_t M / (A_r N_r + A_t M)]}{A_s N_s + A_m D [A_t M / (A_r N_r + A_t M)]}. \quad (59)$$

Finally this Equation can be written in terms of the dose  $D = x t_D$  and by using the previous approximation (39):

$$L(D) = \frac{A_t N_t x}{A_s N_s s_t \exp(-E_t/kT_{irr})} (1 - e^{-(A_s N_s s_t \exp(-E_t/kT_{irr}) / (A_t N_t + A_s N_s)) x D}) \times \frac{A_m A_t M}{A_s N_s (A_r N_r + A_t M)} D. \quad (60)$$

This is the desired analytical equation which expresses the luminescence signal  $L(D)$  measured after the irradiation is carried out at a higher temperature  $T_{irr}$ .

This non-linear function of the dose  $D$  contains explicitly the dose rate  $x$ , indicating that the magnitude of the luminescence signal  $L(D)$  depends also on the dose rate  $x$  used during the irradiation stage. From Eq. (60), as long as the exponent

$$y = \frac{A_s N_s s_t \exp(-E_t/kT_{irr})}{(A_t N_t + A_s N_s) x} D$$

is much smaller than unity, one has  $1 - e^{-y} \approx y$ . Since this exponent includes the dose rate  $x$  in the denominator, it will cancel out with the  $x$  in the preceding term. This means that for short values of the irradiation time  $t = D/x$ , there will be no dose-rate dependence. For longer irradiation times, one would expect a dose-rate effect. This prediction from the analytical Eq. (60) is verified in the next section, by the numerical results obtained from solving the system of differential Eqs. (1–7).

Eq. (60) is most useful for analyzing experimental data when it is written in parametric form as follows:

$$L(D) = k \frac{x}{\exp(-E_t/kT_{irr})} (1 - e^{-\lambda(\exp(-E_t/kT_{irr})/x)D})D. \quad (61)$$

This equation shows clearly the various factors that can be controlled experimentally, namely the irradiation temperature  $T_{irr}$ , the dose rate  $x$  used during irradiation, and the irradiation dose  $D$ . The constants  $k$  and  $\lambda$  in this equation depend only on the kinetic parameters in the model, such as the concentrations  $N_t, N_s$ , etc. and the transition probability coefficients  $A_t, A_s$  etc.

It is also noted that by inserting  $N_r = 0$  in Eqs. (59) or (60), one still obtains similar expressions and the same type of dose behavior, i.e. once more the presence of the reservoir in the model does not affect the behavior of the luminescence signal as a function of the dose  $D$  and a function of the dose rate  $X$ . As mentioned previously in the discussion of Eq. (40), the presence

of the hole reservoir  $R$  in the model only affects the overall magnitude of the luminescence signal in these expressions.

### 5. Numerical results

The parameters chosen for demonstrating the accuracy of the analytical expressions in this paper are similar to those given in Chen and Pagonis [25]. The values used are:  $s_t = 10^{13} \text{ s}^{-1}$ ;  $E_t = 1.0 \text{ eV}$ ;  $s_r = 10^{13} \text{ s}^{-1}$ ;  $E_r = 1.8 \text{ eV}$ ;  $A_t = 10^{-12} \text{ cm}^3 \text{ s}^{-1}$ ;  $A_r = 10^{-9} \text{ cm}^3 \text{ s}^{-1}$ ;  $A_s = 10^{-11} \text{ cm}^3 \text{ s}^{-1}$ ;  $A_m = 10^{-12} \text{ cm}^3 \text{ s}^{-1}$ ;  $A_l = 10^{-12} \text{ cm}^3 \text{ s}^{-1}$ ;  $N_t = 10^{14} \text{ cm}^{-3}$ ;  $N_s = 10^{14} \text{ cm}^{-3}$ ;  $N_r = 2 \times 10^{14} \text{ cm}^{-3}$ ;  $M = 3 \times 10^{14} \text{ cm}^{-3}$ ;  $\chi = 10^9 \text{ cm}^{-3} \text{ s}^{-1}$  and irradiation times  $t_D = 0 - 7 \times 10^5 \text{ s}$  in the example given in this paper.

Fig. 2(a) shows the simulated concentrations of traps and centers during the irradiation stage I. All electron and hole concentrations vary linearly with time. Fig. 2(b) shows the TL/OSL dose response for the chosen set of parameters, and the solid line in this figure represents the quadratic analytical expression (40), while the circles represent the solution of the differential equations in the model. The agreement between the analytical expression and the irradiation time (or dose) is seen to be very good. Fig. 3(a) shows the dose response of the concentrations of trapped electrons and holes during irradiation for longer times, while Fig. 3(b) shows the dose response of the corresponding integrated TL/OSL signal. The inset in Fig. 3(b) shows the same data on a log-log scale, clearly indicating the extent of the quadratic dose response. The dashed line in the inset is added

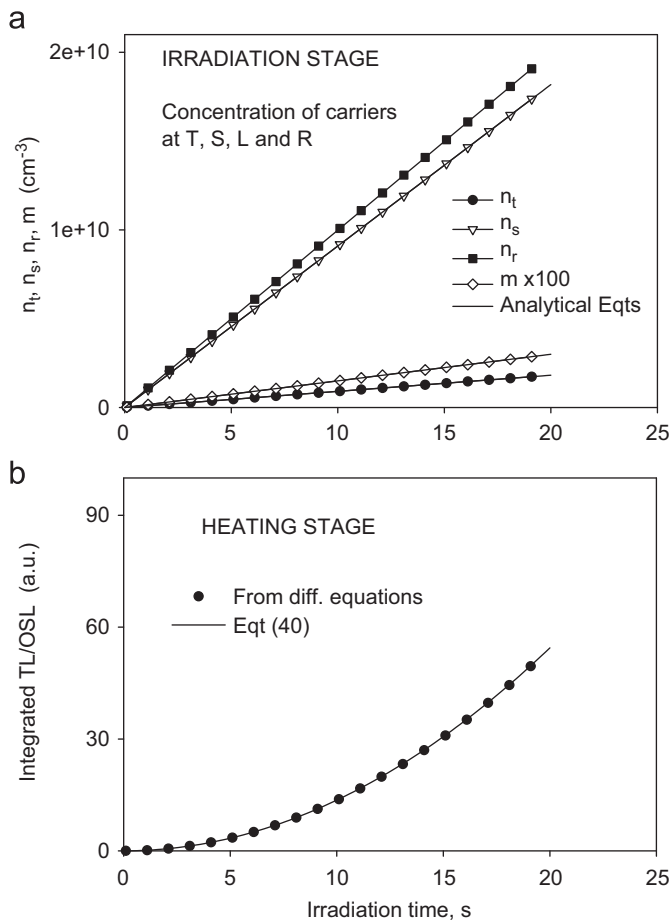


**Fig. 2.** (a) The concentrations of traps and centers during the irradiation stage I described in the text. The parameters are those given in the text, and all electron and hole concentrations vary linearly with time. (b) For the chosen set of parameters, the TL/OSL dose response is quadratic at low doses  $D$ . The solid line represents the analytical expression (40), while the circles represent the solution of the differential equations in the model.

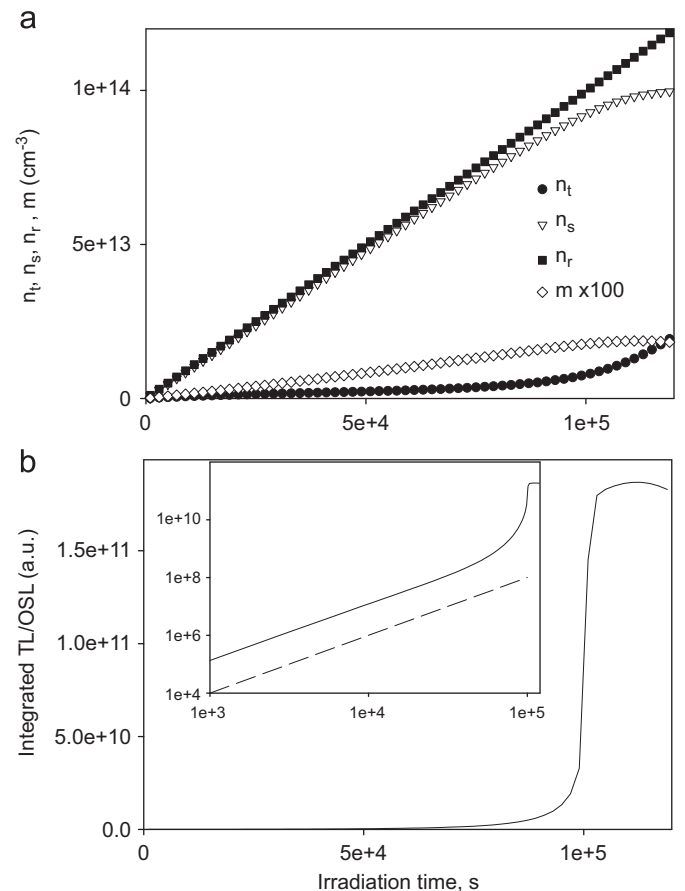


**Fig. 3.** (a) The dose response of the concentrations of traps and holes at large doses. (b) The dose response of the integrated TL/OSL signal at large doses. The inset shows the same data on a log-log scale. The dashed line in the inset is added as a guide to the eye, and represents the quadratic dose response as the 2:1 line on this log-log scale.

as a guide to the eye, and represents the quadratic dose response as the 2:1 line on this log–log scale.

Fig. 3(b) also shows a very strong superlinearity starting at  $t \sim 7 \times 10^4$  s. This more than quadratic superlinearity is associated with the approach of the competitor trap to saturation; as seen clearly in Fig. 3(a), at  $t \sim 7 \times 10^4$  s the concentration of filled competitor traps  $n_s$  is approaching  $N_s$ , and this leads to more electrons being available for the main dosimetric trap. Indeed, the concentration  $n_t$  shows a sharp increase in the region  $t > 7 \times 10^4$  s. This type of behavior is identical to, e.g. the previously reported simulation results by McKeever and Chen [24].

It is emphasized that the degree of superlinearity changes as a function of dose at the different dose-level regions. However, several important dosimetric materials show quadratic super-linear behavior starting at the lowest possible radiation doses after annealing. For example, it is well established by experiment that two important dosimetric materials, quartz and  $\text{Al}_2\text{O}_3\text{:C}$ , have quadratic behavior at low doses after the samples have been annealed. The model in the paper describes this exact quadratic behavior seen at very low doses, and is not applicable for higher dose regions, or for materials which exhibit non-quadratic behavior at low doses. The model is also not meant to describe the dose response at higher dose regions, but rather is strictly applicable for materials exhibiting quadratic dose response at the lowest experimental doses. The simulated data shown in Fig. 3b shows an example of what the dose behavior may look like in the complete range of doses, from the lowest possible experimental doses up to the saturation of the TL/OSL

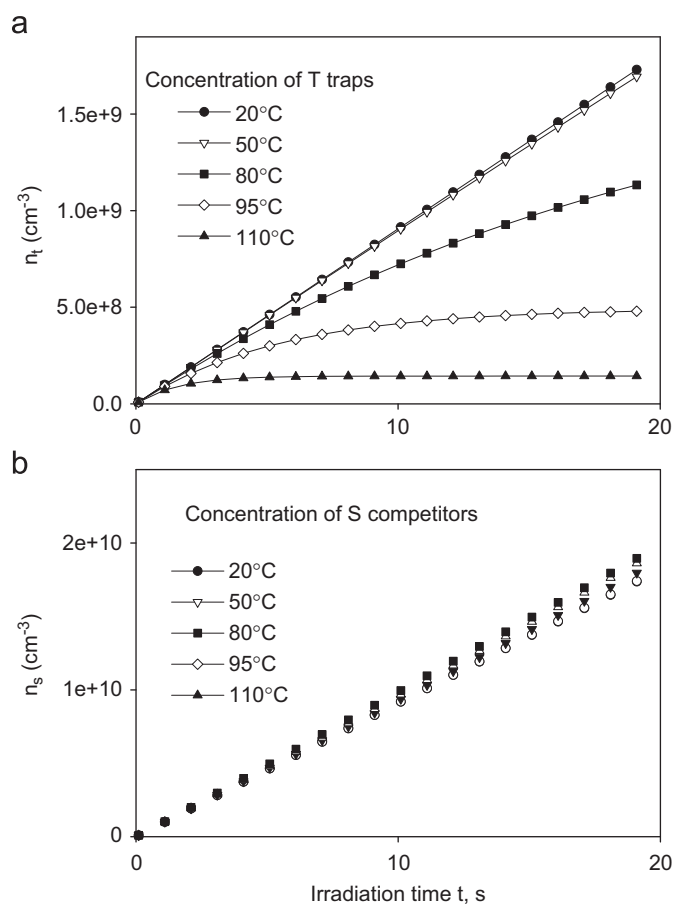


Fig. 4. (a) The dose response of the dosimetric traps  $T$  during irradiation at various elevated temperatures, showing the trap filling process. (b) The dose response of the competitor traps  $S$  during irradiation at elevated temperatures.

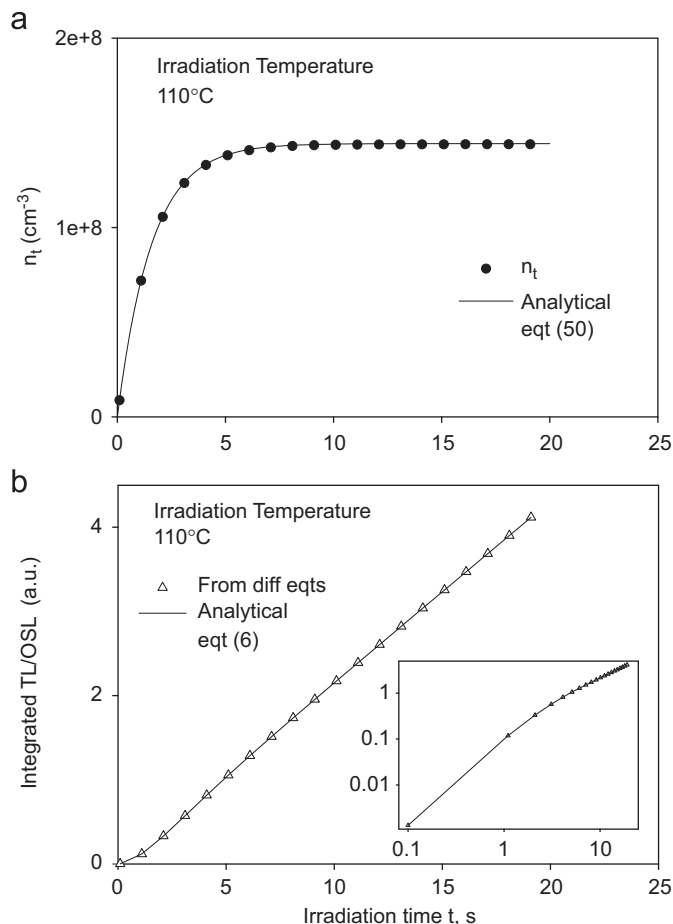


Fig. 5. (a) The dose response of the traps and centers when irradiation takes place at 110 °C. The solid line is the analytical equations. (b) The dose response of the integrated TL/OSL signal when irradiation takes place at 110 °C. The solid line is the solution of the analytical equations. The same data is shown in the inset on a log–log scale.

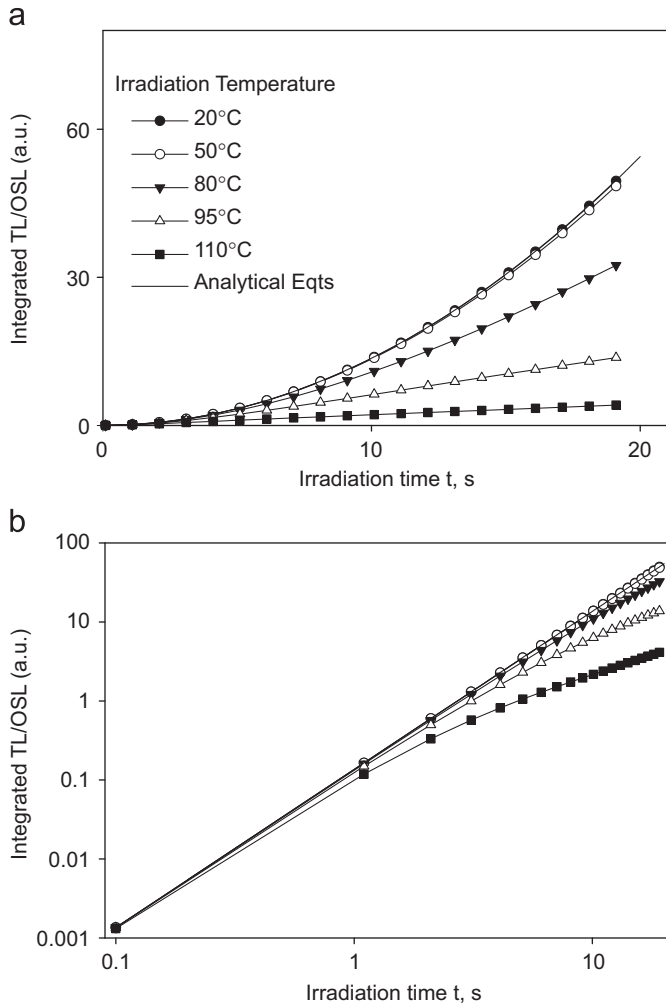
signal. The equations derived in this paper are applicable only at the lowest dose region shown in Fig. 3b.

Fig. 4(a) shows the dose response of the dosimetric traps  $T$  during irradiation at various elevated temperatures, showing the non-linear trap filling process. Fig. 4(b) shows the corresponding concentrations of the competitor trap  $S$ . The concentration of holes in the  $L$  centers during irradiation is not affected and remains constant at the elevated temperatures.

Fig. 5(a) shows a specific example of the dose response of the traps and centers when irradiation takes place at 110 °C, while Fig. 5(b) shows the dose response of the integrated TL/OSL signal when irradiation takes place at this elevated temperature. The inset of Fig. 5(b) shows the same data on a log–log scale, indicating more clearly the range of doses in which the super-linear behavior is observed. All solid lines in Fig. 5 represent the corresponding analytical equations.

Fig. 6(a) shows the dose response of the integrated TL/OSL signal when irradiation takes place at several elevated temperatures, with the solid lines representing once more the analytical Eq. (60). Fig. 6(b) shows the same data as Fig. 6(a), on a log–log scale. The effect of the elevated irradiation temperature on the quadratic/superlinear dose dependence is clearly seen at the various irradiation temperatures.

Fig. 7(a) shows the dose-rate effect discussed in the previous section, for an irradiation temperature of 110 °C. This effect was predicted on the basis of Eq. (60). The dose rate  $x$  is varied within two orders of magnitude, from  $x = 10^7 \text{ cm}^{-3} \text{ s}^{-1}$  to



**Fig. 6.** (a) The dose response of the integrated TL/OSL signal when irradiation takes place at several elevated temperatures. The solid lines are from the analytical equations. (b) The same data as in (a), on a log–log scale. The quadratic/superlinear dose dependence is clearly seen at low irradiation times.

$\chi = 10^9 \text{ cm}^{-3} \text{ s}^{-1}$ . For each point in Fig. 7 corresponding to a fixed dose  $D = \chi t$ , the corresponding irradiation time is varied inversely proportional to  $\chi$ , so that the total doses to the sample are kept at constant values  $D = \chi t$ . The solid lines in Fig. 7 represent the analytical Eq. (60). The effect of the dose rate on the quadratic dose dependence is clearly seen at higher doses in Fig. 7(b). At small doses  $D$  all curves in Fig. 7(b) coincide, and there is no dose-rate dependence, as discussed previously. The dashed line in the Fig. 7(b) is added as a guide to the eye, and represents the quadratic dose response as the 2:1 line on this log–log scale.

An additional observation from the results of Fig. 7(b), is that in the case of low dose rates (solid circles,  $\chi = 10^7 \text{ cm}^{-3} \text{ s}^{-1}$ ) the quadratic superlinearity extends over the whole dose region, while at high dose rates (open circles,  $\chi = 10^9 \text{ cm}^{-3} \text{ s}^{-1}$ ) the superlinearity is limited to very low doses.

On the basis of Figs. 6 and 7, and based on analytical Eq. (60), it is concluded that the superlinearity effects discussed in this paper will depend on both the irradiation temperature and on the dose rate used during these experiments.

## 6. Discussion

Kristianpoller et al. [22] considered a kinetic model of two competing traps and one recombination center (two-trap

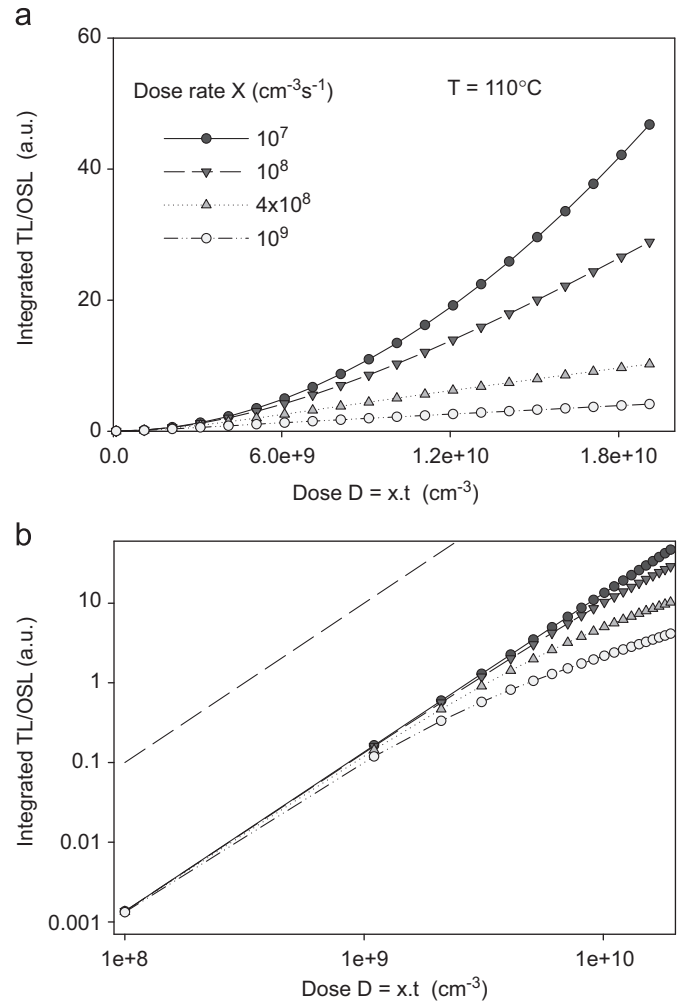


**Fig. 7.** (a) The dose response of the integrated TL/OSL signal when irradiation takes place at an elevated temperature of 110 °C, and at different dose rates  $\chi$ . For each point corresponding to a certain dose  $D = \chi t$ , the irradiation times used at each dose rate are taken to be inversely proportional to  $\chi$ , so that the total dose  $D = \chi t$  remains constant. The solid lines are calculated from the analytical equations. (b) The same data as in (a), on a log–log scale. The quadratic/superlinear dose dependence is clearly seen at low irradiation doses. The dashed line is added as a guide to the eye, representing the quadratic dose response as the 2:1 line on this log–log scale.

one-center, or 2T1C model) and showed that the area  $L$  under the glow peak is given approximately by

$$L = \frac{A_m m_0 n_0}{A_2 N_2}, \quad (62)$$

where  $A_2 (\text{cm}^3 \text{ s}^{-1})$  is the trapping coefficients into the competitor trap of concentration  $N_2 (\text{cm}^{-3})$ , and  $A_m (\text{cm}^3 \text{ s}^{-1})$  is the recombination coefficient of electrons in the conduction band. In this expression  $m_0$  and  $n_0$  represent the concentrations of holes in the recombination center and electrons in the dosimetric trap correspondingly, at the end of the irradiation period. This expression yields the quadratic dose dependence reported by Rodine and Land [50], if both  $m_0$  and  $n_0$  are linear functions of the irradiation dose.

Eq. (62) can be compared directly with Eq. (35) derived in this paper:

$$L = (n_t)_I \frac{A_m(m)_{II}}{A_s N_s + A_m(m)_{II}} = (n_t)_I \frac{A_m(m)_I}{A_s N_s + A_m(m)_I} \simeq \frac{A_m(m)_I (n_t)_I}{A_s N_s}, \quad (35')$$

where we used the previous approximation  $A_s N_s \gg A_m m_l$  and  $(m)_{II} = (m)_I$ .

This shows that Eq. (62) in this paper (previously derived by Kristianpoller et al. [22]), is exactly equivalent to Eq. (40) derived in this paper. However, Eq. (40) has the following advantages: (a) it contains only the kinetic parameters of the model and (b) contains explicitly the experimental irradiation dose  $D$ .

Furthermore, in this paper the more general Eq. (61) was derived, for the situation in which irradiation of the sample takes place at an elevated temperature.

A survey of the TL/OSL literature shows that there are very few experimental TL/OSL studies in which irradiation of the luminescence material takes place at elevated temperatures. The only published studies of this type that we are aware of, are the TL papers by Charitidis et al. ([7,8]), on synthetic and natural quartz samples; several of these studies concern the well-known 110 °C TL peak of quartz. Unfortunately, most of the irradiations for these experiments were performed mostly at very low temperatures, well-below room temperature. In addition, the dose ranges used in these experiments do not overlap with the low doses necessary for the model to be applicable. In total, it is not possible to compare these published experiments directly with the superlinearity model in this paper.

Further experimental work in this area is necessary in order to carry out a direct comparison with the model.

It is also worth mentioning that the dose-rate effect predicted on the basis of Eq. (60) should be observable only at elevated irradiation temperatures, and that the model predicts no dose rate effect when irradiation takes place at room temperature. Furthermore, the predicted dose rate effect is rather large; the simulated data of Fig. 7 shows a change in the emitted TL/OSL signal by almost an order of magnitude. There have been published experimental reports of dose-rate effects for TL/OSL signals, in which the typical change of the luminescence signal is by up to a factor of  $\sim 2$  (see for example, [25] chapters 7 and 8). However, these reported experimental dose-rate effects should be of a different nature than the dose-rate effect predicted here, since they are observed experimentally when irradiation takes place at room temperature.

At first it may appear that some of the assumptions made in the derivation of the equations in this paper are far from reality. For example, the model assumes an absence of significant recombinations during the irradiation stage, and also assumes an absence of significant non-radiative recombinations during the two stages of irradiation and heating. In order to investigate the possible effect of these assumptions on the derived results, we have repeated these simulations and analytical derivations using a recently published comprehensive model for quartz (Pagonis et al. [33,51,52]). This model consists of 7 electron traps and 4 hole centers, and has been used successfully to simulate a variety of TL/OSL phenomena in quartz, including the quadratic dose response at low doses (Pagonis et al. [33]).

Our simulations using this comprehensive model show that the superlinearity effects described in this paper are also present when using this more comprehensive model. Furthermore, it is found that simulated irradiation at higher temperatures does indeed result in the same type of variable superlinearity effect in quartz, similar to the behavior demonstrated in this paper. New analytical equations derived using the comprehensive model of Pagonis et al. [33,51,52] are found to be in good agreement with the simulated results from the model. In view of these additional simulated results, we believe that the results derived in this paper are of more general applicability than it appears at first glance. The results of these additional simulations are beyond the scope of this paper, and will be presented elsewhere.

As mentioned above, the equations derived in this paper are applicable only at the lowest dose region shown in Fig. 3b. This

figure shows that at higher doses the dose response has a superlinearity coefficient greater than 2, leading up to the saturation region. To the best of our knowledge, there are no analytical solutions describing this superlinearity greater than 2 in the literature. This higher-than-quadratic superlinear behavior has been demonstrated convincingly by simulation in reference [22].

## 7. Conclusions

In this paper analytical equations were derived for the well-known superlinear dose response of TL/OSL signals in annealed samples. The main assumptions made during the derivation are the quasi-equilibrium (QE) conditions, low irradiation doses and weak recombination processes. The derived analytical expression (40) in this paper contains only the kinetic parameters in the model, and the irradiation dose  $D$ . The more general analytical Eqs. (60) and (61) derived here extend Eq. (40) to the case of irradiation taking place at elevated temperatures. The analytical expression (61) can be used directly to analyze and parameterize the dose response of luminescence materials, when irradiation takes place at elevated temperatures.

## References

- [1] A. Halperin, R. Chen, *Phys. Rev.* 148 (1966) 839.
- [2] H. Otaki, H. Kido, A. Hiratsuka, Y. Fukuda, N. Takeuchi, *J. Mater. Sci. Lett.* 13 (1994) 1267.
- [3] T. Mikado, T. Tomimasu, T. Yamazaki, M. Chiwaki, *Nucl. Instrum. Meth.* 157 (1978) 109.
- [4] T. Yamazaki, T. Tomimasu, T. Mikado, M. Chiwaki, *J. Appl. Phys.* 49 (1978) 4929.
- [5] I.I. Matrosov, Yu.L. Pogorelov, *J. Appl. Spect.* 29 (1978) 1327.
- [6] C. Felix, A.K. Singhvi, *Radiat. Meas.* 27 (1997) 599.
- [7] C. Charitidis, G. Kitis, C. Furetta, S. Charalambous, *Radiat. Prot. Dosim.* 84 (1999) 95.
- [8] C. Charitidis, G. Kitis, C. Furetta, S. Charalambous, *Nucl. Inst. Meth. Phys. Res. B* 168 (2000) 404.
- [9] J. Zimmerman, *C Phys., Solid State Phys.* 4 (3265) (1971) 3277.
- [10] E. Piesch, B. Burgkhardt, A.M. Sayed, *Proc. Int. Conf. Lumin. Dosim. Krakow* (1974) 1201.
- [11] M.C. Wintersgill, P.D. Townsend, *Radiat. Eff. Def. Sol.* 38 (1978) 113.
- [12] I. Nail, Y.S. Horowitz, L. Oster, M.E. Brandan, M. Rodriguez-Villafuerte, A.E. Buenfil, C. Ruiz-Trejo, I. Gamboa-deBuen, O. Avila, V.M. Tovar, P. Olko, N. Ipe, *Radiat. Prot. Dosim.* 119 (2006) 180.
- [13] P.V. Mitchell, D.A. Wiegand, R. Smoluchowski, *Phys. Rev.* 121 (1961) 484.
- [14] A. Wieser, H.Y. Göksu, D.F. Regulla, A. Waibel, *Nucl. Tracks Radiat. Meas.* 18 (1991) 175.
- [15] A.R. Lakshmanan, K.G. Vohra, *Nucl. Instrum. Meth.* 159 (1979) 585.
- [16] X.B. Yang, J. Xu, H.J. Li, Q.Y. Bi, Y. Cheng, Q. Tang, *J. Appl. Phys.* 106 (2009) 033105.
- [17] D.I. Godfrey-Smith, *J. Phys. D: Appl. Phys.* 27 (1994) 1737.
- [18] R.G. Roberts, N.A. Spooner, D. Questiaux, *Radiat. Meas.* 23 (1994) 647.
- [19] L. Bøtter-Jensen, N. Agersap Larsen, V. Mejdahl, N.R.J. Poolton, M.F. Morris, S.W.S. McKeever, *Radiat. Meas.* 24 (1995) 535.
- [20] E.G. Yukihara, V.H. Whitley, S.W.S. McKeever, A.E. Akselrod, M.S. Akselrod, *Radiat. Meas.* 38 (2004) 317.
- [21] R. Chen, S.W.S. McKeever, *Theory of Thermoluminescence and Related Phenomena*, World Scientific, Singapore, 1997., p. 208.
- [22] N. Kristianpoller, R. Chen, M. Israeli, *J. Phys. D: Appl. Phys.* 7 (1974) 1063.
- [23] R. Chen, X.H. Yang, S.W.S. McKeever, *J. Phys. D: Appl. Phys.* 21 (1988) 1452.
- [24] S.W.S. McKeever, R. Chen, *Radiat. Meas.* 27 (1997) 625.
- [25] R. Chen, V. Pagonis, *Thermally and Optically Stimulated Luminescence: A Simulation Approach*, Wiley and Sons, Chichester, 2011.
- [26] R. Chen, P.L. Leung, *Radiat. Meas.* 33 (2001) 475.
- [27] R. Chen, S.G.E. Bowman, *Eur. PACT J.* 2 (1978) 216.
- [28] R. Chen, S.W.S. McKeever, *Radiat. Meas.* 23 (1994) 667.
- [29] R. Chen, P.L. Leung, *J. Appl. Phys.* 89 (2001) 259.
- [30] D. Banerjee, M. Blair, S.W.S. McKeever, *Radiat. Prot. Dosim.* 101 (2002) 353.
- [31] D. Banerjee, *Radiat. Meas.* 33 (2001) 47.
- [32] R.M. Bailey, *Radiat. Meas.* 33 (2001) 17.
- [33] V. Pagonis, R. Chen, G. Kitis, *J. Archaeol. Sci.* 38 (2011) 1591.
- [34] F.A. Savikhin, *J. Appl. Spect.* 17 (1972) 889.
- [35] G.S. Zavit, F.A. Savikhin, *Izv. Akad. Nauk SSSR, Ser. Fiz.* 38 (1974). 1325 (p. 190 in the English translation).
- [36] L.N. Kantorovich, G.M. Fogel, V.I. Gotlib, *J. Phys. D: Appl. Phys.* 21 (1988) 1008.

- [37] C.M. Sunta, R.N. Kulkarni, E.M. Yoshimura, A.W. Mol, T.M. PETERS, E. Okuno, *Phys. Status Solidi B* 186 (1994) 199.
- [38] F. Mady, D. Lapraz, P. Iacconi, *Radiat. Meas.* 43 (2008) 180.
- [39] J. Faïn, M. Monnin, *J. Electrostat.* 3 (1977) 289.
- [40] J. Faïn, S. Sanzelle, D. Miallier, M. Monret, Th. Pillere, *Radiat. Meas.* 23 (1994) 287.
- [41] C.K. Lee, R. Chen, *J. Phys. D: Appl. Phys.* 28 (1995) 408.
- [42] R. Chen, P.L. Leung, *Radiat. Prot. Dosim.* 84 (1–4) (1999) 43.
- [43] R. Chen, V. Pagonis, *J. Phys. D: Appl. Phys.* 37 (2004) 159.
- [44] C.K. Lee, H.K. Wong, Y.L. Leung, *Radiat. Meas.* 44 (2009) 215.
- [45] V. Pagonis, R. Chen, J.L. Lawless, *Radiat. Meas.* 43 (2008) 175.
- [46] V. Pagonis, R. Chen, J.L. Lawless, *Radiat. Meas.* 42 (2007) 198.
- [47] M. Figel, C. Goedicke, *Radiat. Prot. Dosim.* 84 (1–4) (1999) 433.
- [48] V. Pagonis, G. Kitis, R. Chen, *Radiat. Meas.* 37 (2003) 267.
- [49] V. Pagonis, J.L. Lawless, R. Chen, C. Andersen, *J. Phys. D: Appl. Phys.* 42 (2009) 175107.
- [50] E.T. Rodine, P.L. Land, *Phys. Rev. B* 4 (1971) 2701.
- [51] V. Pagonis, A.G. Wintle, R. Chen, X.L. Wang, *Radiat. Meas.* 43 (2008) 704.
- [52] V. Pagonis, A.G. Wintle, R. Chen, X.L. Wang, *Radiat. Meas.* 44 (2009) 634.